Guest Orientation in Uniplanar-Axial Polymer Host Films and in Co-Crystal Unit-Cell, Determined by Angular Distributions of Polarized Guest Fluorescence

Hideyuki Itagaki,* Tomohiro Sago, Miho Uematsu, and Genki Yoshioka

Department of Chemistry, Graduate School of Electronic Science and Technology and School of Education, Shizuoka University, 836 Ohya, Suruga-ku, Shizuoka, 422-8529, Japan

Andrea Correa, Vincenzo Venditto, and Gaetano Guerra*

Dipartimento di Chimica and INSTM Research Unit, Università degli Studi di Salerno, via Ponte Don Melillo, I-84084 Fisciano (SA), Italy

Received August 13, 2008; Revised Manuscript Received September 26, 2008

ABSTRACT: Syndiotactic polystyrene (sPS) films with uniplanar-axial orientation of their co-crystalline phase with a fluorescent guest (naphthalene, NP) have been prepared and the orientation of their crystalline phase has been fully characterized by X-ray diffraction measurements. The prepared films have been examined in detail using Nishijima's method, where angular distribution of NP polarized fluorescence intensities was measured at each setting film angle by the rotation of films around the excitation light beam. This polarized fluorescence method turns out to be quite effective for monitoring the orientation of fluorescent guest molecules in the films. In particular, in semicrystalline films presenting uniplanar-axial orientation of their sPS/NP clathrate phase, NP molecules were found to exhibit a high three-dimensional orientational order all over the films. The experimental data have also allowed to determine the orientation of the NP guest molecule with respect the axes of the co-crystal unit-cell: in satisfactory agreement with molecular modeling results, angles formed by the short and the long axes of NP with the *c* axis are not far from 80° while the angle between the short axis of NP and the *a* axis is nearly 105°.

Introduction

Fluorescence spectroscopy is growing remarkably as a powerful and effective tool to study the physical and chemical behaviors of macromolecules.[1−3] Because fluorescence techniques are not only highly sensitive but also nondestructive, they are useful for monitoring changes in the microenvironment whatsoever. Thus far, however, fluorescence techniques have not been employed so effectively for studies on polymer crystal systems. We therefore have applied fluorescence techniques to the studies on the microenvironments in crystalline and amorphous regions of polymer molecules[4−7] or on molecules being the guest of a polymer co-crystal.[8]

Polarized fluorescence measurements are considered to be a quite effective method for determining the possible regular orientation of a chromophore in polymer films. Nishijima[9] reported the way of measuring the polarized fluorescence of chromophores doped in plastic films by rotating the sample around the excitation light beam, as shown in the section of the method in the present paper. He claimed that this method can clarify orientation of fluorescent chromophores that cannot be discriminated from infrared dichroism measurements, because infrared dichroism monitors only the absorption change while the polarized fluorescence method is related to not only absorption of polarized light but also detection of polarized fluorescence, thus, its intensity reflects the arrangement of a chromophore more exactly against two different standard axes. However, in spite of the method being so sophisticated, unfortunately, no adequate samples where the arrangement of guest fluorescent chromophores is three-dimensionally highly ordered in plastic films or crystals have been available. As a consequence, the efficiency of this method has not been demonstrated so far.

In this paper we show that polymer films with nanoporous and co-crystalline phases presenting a uniplanar-axial orientation are particularly suitable for the Nishijima's method and, hence, allow to determine the fluorescent guest orientation with respect to the film plane as well as with respect to the crystalline axes of the polymeric host framework.

Polymeric co-crystalline phases are quite common for several regular and stereoregular polymers, for example, syndiotactic polystyrene (sPS),[10,11] syndiotactic poly(*p*-methylstyrene),[12] syndiotactic poly(*p*-chlorostyrene),[13] poly(muconic acid),[14] or polyethyleneoxide.[15] The crystalline structures of several polymer co-crystals have been determined, generally by X-ray diffraction measurements on axially oriented films and fibers. This procedure, for the case of well-ordered polymer co-crystals, allows determining with a good accuracy the guest location and orientation with respect to the axes of the crystalline phases.

In most cases, the removal of the low-molecular-mass guest molecules from these polymer co-crystals generates host chain rearrangements generally leading to crystalline phases that, as usual for polymers, exhibit a density higher than that one of the corresponding amorphous phase.

For the case of sPS[16] (and of sPS-based copolymers),[13,17] by using suitable guest removal techniques,[18] two different nanoporous crystalline phases (δ[19] and ε[20]), exhibiting a density ($\rho = 0.98$ g/cm^3) definitely lower than that of the amorphous sPS ($\rho = 1.05$ g/cm^3), can be obtained. The empty space is organized as isolated cavities and channels, for δ and ε crystalline phases, respectively. In particular, the δ form is monoclinic (space group $P2_1/a$; $a = 1.74$ nm; $b = 1.18$ nm; $c = 0.78$ nm; $\gamma = 117°$) and exhibit per unit cell two identical cavities centered on the center of symmetry and bounded by 10 phenyl rings.[19a,b]

* To whom correspondence should be addressed. Phone: +81-54-2384627(H.I.). Fax: +81-54-2373354 (H.I.). E-mail: edhitag@ipc.shizuoka.ac.jp (H.I.); gguerra@unisa.it (G.G.).

10.1021/ma801849b CCC: $40.75
Published on Web 11/06/2008

These nanoporous phases are able to absorb, also from diluted solutions[21] or from gas phases,[22] low-molecular-mass guest molecules occupying also only a fraction of its crystalline cavities. When the degree of occupancy of the crystalline cavities is low, due to the intrinsic crystalline disorder, the X-ray diffraction method is not able to give information relative to the guest location and orientation.

On the other hand, we have shown that infrared linear dichroism measurements on uniaxially oriented films allow to establish the orientation of the guest molecules with respect to the host chain axis, also for the case of relatively low degree of occupancy of the cavities.[8,23] However, these linear dichroism measurements are not able to give information on the orientation of the guest molecules with respect to the other axes of the host polymeric phase.

As for the orientation of the host polymeric crystalline phase, recent studies on sPS films have shown that, besides the usual axial orientation, which can be achieved for all the different crystalline phases,[24] three different kinds of uniplanar orientations have been developed for the helical crystalline forms (γ, δ, ε, and co-crystalline forms).[25−27] In particular, as for the nanoporous δ phase, it is possible to prepare films with $a_{\parallel}\, c_{\parallel}$[25] or $a_{\perp}\, c_{\parallel}$[26] or $a_{\parallel}\, c_{\perp}$[27] uniplanar orientations.

In the present paper we show that it is possible to prepare sPS films exhibiting both $a_{\parallel}\, c_{\parallel}$ uniplanar and axial orientations (the so-called uniplanar-axial orientation),[28] both for the nanoporous δ phase as well as for the co-crystalline (clathrate)[8] phase with NP.

Films presenting uniplanar-axial orientation of the sPS δ phase and including different amounts of NP guest molecules have been examined by using Nishijima's method, where angular distribution of NP polarized fluorescence intensities was measured, at each setting film angle by the rotation of films around the excitation light beam. It is shown that experimental fluorescence data allow determining the three-dimensional orientational order of an NP molecule in the film as well as in the polymer host unit-cell, also for low degree of occupancy of the cavities of the δ phase.

A precise determination of the orientation of the guest molecules with respect to the surface of also macroscopic films is particularly relevant in view of the advanced applications proposed for sPS films, not only as fluorescent materials,[8] but also as optical[29] and chiro-optical[30] memories and as non-linear-optical materials.[31]

Method of the Polarized Fluorescence Measurements by Rotating a Sample around the Excitation Light. First we show our method to measure polarized fluorescence of a chromophore and its angle distribution and explain how the orientation of a chromophore is related to its polarized fluorescence.

Figure 1 demonstrates the general measurement of polarized fluorescence of a sample. Light is a moving wave vibrating vertically against the direction of progress. Iv and Ih, which are unit vectors of electric field for the polarized light, are shown in the figure together with the setting way of a polarizer to produce a polarized light whose vector of electric field is Iv or Ih. Two sets of polarizers are used for the measurements: polarizer 1 is always set as Iv to produce the same polarized light as the excitation light of a sample. The polarizer 2 is set in front of the detector as is shown to be either parallel (Iv) or vertical (Ih) to polarizer 1. The fluorescence intensity of a sample is defined to be I0 and I90 when polarizer 2 (fluorescence) is set as Iv and Ih, respectively. I0 and I90 are dependent on how much a sample absorbs the polarized excitation light and how much its polarized fluorescence can go through the polarizer 2.

In general, when a chromophore is excited by polarized light, the emission of the chromophore will be observed to be

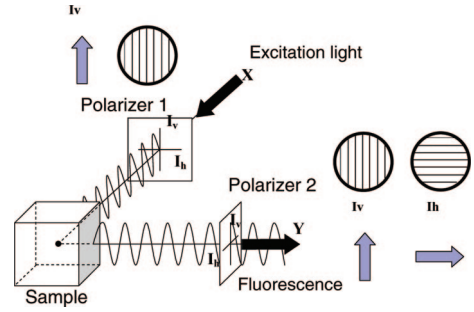

Figure 1. Sketch of polarized fluorescence measurements. Iv and Ih are unit vectors of electric field for the polarized light selected by a polarizer. Polarizer 1 is set as to choose a polarized light whose vector of electric field is Iv as the excitation light, while polarizer 2 are automatically set to be either parallel or vertical to polarizer 1.

polarized if (I) the molecular motion of the chromophore is slow enough and (II) energy transfer and energy migration do not take place. The fluorescence anisotropy, r, which is defined as eq 1, is convenient for evaluation of how much the fluorescence is polarized.

$$r = (\mathrm{I0} - G \times \mathrm{I90})/(\mathrm{I0} + 2G \times \mathrm{I90}) \tag{1}$$

where G is a machine constant obtained as i90/i0: i0 and i90 are the fluorescence intensities when polarizer 1 is fixed as Ih and polarizer 2 (fluorescence) is set as Ih and Iv, respectively. Usually the comparison between r values is efficient for obtaining information about the molecular motions and energy transportation of fluorescent molecules in a system.

We can estimate I0 and I90 of a chromophore in a film. Here the transition moments for absorption and fluorescence of a chromophore are described to be $\boldsymbol{\mu}_{\mathrm{A}}$ and $\boldsymbol{\mu}_{\mathrm{F}}$, respectively. Let us imagine that all the chromophores, being isolated from each other, have the same arrangement in a film and their molecular motions are restricted perfectly. We define the angle between $\boldsymbol{\mu}_{\mathrm{A}}$ of the chromophore and the Iv of excitation light to be α (degree) and the angle between $\boldsymbol{\mu}_{\mathrm{F}}$ and the Iv (of polarizer 2 (fluorescence)) to be β (degree). If a chromophore is excited at a wavelength of the first absorption band according to the transition to the lowest excited state, namely, from S_0 to S_1, β is identical with α. However, we can change $\boldsymbol{\mu}_{\mathrm{A}}$, namely, α, by changing excitation light wavelength to be shorter. Here the intensity for a chromophore in the film to absorb the excitation light shown as Iv is proportional to $\cos^2 \alpha$, while the possibility for the polarized fluorescence of the chromophore able to pass through polarizer 2 is proportional to $\cos^2 \beta$. Thus, the intensity of I0 monitored by the detector at the back of polarizer 2 is given by eq 2.

$$\mathrm{I0} = K\Phi \cos^2 \alpha \cos^2 \beta \tag{2}$$

where K is the maximum probability of excitation attainable when the molecular axis of the chromophore coincides with the direction of Iv of excitation light and Φ is the energy yield of fluorescence. I90 is obtained for the polarized fluorescence able to go through polarized 2 when it is set as Ih, namely, perpendicular to the case to monitor I0. Because the angle between $\boldsymbol{\mu}_{\mathrm{F}}$ and Ih (of polarizer 2 (fluorescence)) is to be $90 - \beta$ (degree) in this case, I90 is given by eq 3.

$$\mathrm{I90} = K\Phi \cos^2 \alpha \sin^2 \beta \tag{3}$$

We can know the transition moments for absorption and fluorescence of a chromophore, $\boldsymbol{\mu}_{\mathrm{A}}$ and $\boldsymbol{\mu}_{\mathrm{F}}$, however, α and β are dependent on three-dimensional position of the chromophore against Iv and Ih. Thus, it is obvious that the measurement of I0 and I90 for one position of the film is not enough for

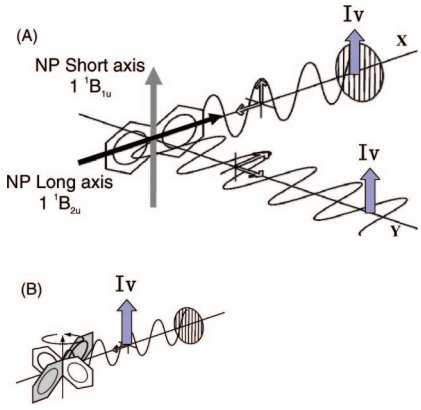

Figure 2. Sketch of absorption and fluorescence of naphthalene (NP). Transition moment of NP, 1 $^1B_{1u}$, to absorb 280 nm light is parallel to the short axis of NP, while transition moment of NP, 1 $^1B_{2u}$, of fluorescence is parallel to the long axis of NP. If an NP molecule has an arrangement against Iv shown in (A), I0 is 0 and I90 has a maximum value. All the NP molecules whose short axes are parallel to Iv can absorb the polarized light most shown in (B).

determining the arrangement of the chromophore even if the arrangement of all the chromophores is unique and the same.

Then, Nishijima et al.[9] introduced the smart method to determine the arrangement of chromophores in a film. It is the method to measure each I0 and I90 of the chromophore by rotating the sample film around the excitation light beam by every 10 or some degrees. This rotation increases the information about the arrangement of the chromophores in a film. At each position of the rotation, because the angles between the transition moments ($\boldsymbol{\mu}_A$ and $\boldsymbol{\mu}_F$) and the three vectors of electric field (Iv of the excitation and Iv and Ih of the fluorescence) must change, we can have the information of precise arrangement of chromophores three dimensionally. Accordingly, these three vectors of electric field can be used as the standard coordinates.

Thus, if we can specify the three-dimensional arrangement of a guest chromophore in a film, we can calculate I0 and I90 of the chromophore no matter how the film is set around the exitation light. Or if the arrangement of a guest molecule is unique, we can estimate the arrangement by reproducing all the I0 and I90 values obtained by rotating the sample.

Just as an example, we show a case where all the NP molecules are oriented, such as in Figure 2. When an NP molecule is excited at 280 nm, which corresponds to the transition from S_0 to S_2, the $\boldsymbol{\mu}_A$ of NP is parallel to the short axis of NP. The fluorescence peaks of NP appear at 325 and 337 nm, corresponding to the transition from S_1 to S_0. This fluorescence transition moment, $\boldsymbol{\mu}_F$, is parallel to the long axis of NP. Thus, in the case where an NP molecule is oriented with high regularity, such as in Figure 2A, this molecule absorbs with the highest probability the polarized excitation light whose vector of electric field is Iv. However, the I0 value must be 0 because the vector of its polarized fluorescence is perpendicular to Iv of polarizer 2; namely, the angle β in this case becomes 90°, giving cos β to be 0. On the contrary, the I90 value is expected to be the highest, because the angle β in this case becomes 0°, giving cos β to be 1, the maximum value. Note that what we have to pay attention to is only the direction of the long and short axes of NP, that is to say, the direction of $\boldsymbol{\mu}_A$ and $\boldsymbol{\mu}_F$ against Iv and Ih. When irradiated at 280 nm, any NP rings at any angles shown in Figure 2B can be excited identically, namely, with the highest probability, because $\boldsymbol{\mu}_A$ of all the NP molecules shown in Figure 2B is parallel to the vector of electric field of the excitation light, that is, $\alpha = 0$ and cos $\alpha = 1$. Moreover, polarized fluorescence emits towards any directions keeping the parallel vibration to the $\boldsymbol{\mu}_F$ of NP. Thus, any fluorescence from the NP in Figure 2A proceeds towards all the directions in the *yz* plane. After the measurements of I0 and I90 of NP at the position shown in Figure 2, the film is rotated around the excitation light beam by every 10 degree, inducing the changes of any angles between the transition moments, namely, the direction of the short and long axes of NP and the vectors of electric field, Iv and Ih, resulting that I0 and I90 come to show different values from those obtained at the position shown in Figure 2A.

Table 1. Characterization of sPS/NP Clathrate Crystalline Films Used in the Present Paper

sample	crystallinity, %	thickness, μm	content of NP, %	stretching
UP1	35−45	32	2.4	×
UP2		45	7	×
UPA1		30	5	○
UPA2		40	5	○

Experimental Section

Materials. To monitor the behavior of polarized fluorescence of NP randomly and uniformly distributed in amorphous films, we prepared (i) atactic polystyrene (aPS) films doped with NP and (ii) atactic poly(vinyl acetate) (PVAc) films doped with NP. aPS films containing NP were prepared on quartz disks by using a spin-coating method from a 4 wt/wt% THF solution of aPS (Tosoh corp.; $M_w = 9.64 \times 10^4$, $M_w/M_n = 1.01$) having 5.0 wt/wt% of NP per aPS and dried by extensive pumping under vacuum for more than 3 days at 40°C. More than four films were prepared to ascertain the reproducibility. The films were left on the quartz disks for ease of handling during subsequent measurements. PVAc films containing 0.24 wt/wt% of NP per PVAc were prepared by casting THF solution of PVAc (Wako Co.) with NP on glass at room temperature for 2 days and dried by extensive pumping under vacuum for more than 3 days at 40°C.

Films UP1, UP2, UPA1, and UPA2 are sPS films, including NP, prevailingly as a guest in their nanoporous δ crystalline phase. The characterization of these films is summarized in Table 1. sPS was supplied by Dow Chemical under the trademark Questra 101. ^{13}C nuclear magnetic resonance characterization showed that the content of syndiotactic polystyrene triads was over 98%. The weight-average molar mass obtained by gel permeation chromatography (GPC) in trichlorobenzene at 135°C was found to be $M_w = 3.2 \times 10^5$ with the polydispersity index, $M_w/M_n = 3.9$.

UP1 and UP2 films were prepared as follows: chloroform clathrate sPS films were first prepared by casting from a 1 wt/wt% sPS solution in chloroform at room temperature. Chloroform guest molecules were replaced by NP, by exposure to NP vapors at room temperature. As described in detail in Results and Discussion, the UP1 and UP2 films present the $a_{||}$ $c_{||}$ uniplanar orientation of the co-crystalline polymer phase.

UPA1 and UPA2 were prepared as follows:[8] first, unoriented amorphous sPS films were obtained by extrusion of the melt sPS at 300°C with an extrusion head of 200 × 0.5 mm. These films were uniaxially stretched at a draw ratio of $\lambda \approx 3$, at a constant deformation rate of 0.1 s^{-1}, in the temperature range of 105−110 °C, with a Brukner stretching machine. During the stretching procedure, the lateral size of the film has been maintained constant by suitable gripping. UPA1 and UPA2 have been obtained by exposure of the axially stretched films to NP vapors at 60°C. As described in detail in Results and Discussion, the UPA1 and UPA2 films present the $a_{||}$ $c_{||}$ uniplanar-axial orientation of the polymer co-crystalline phase.

We would like to comment on the fraction of NP molecules in co-crystalline phase. The guest diffusivity is generally much higher in the amorphous phase than in the co-crystalline phase, as well established with several sPS guest molecules.[21−23] This offers the opportunity to prepare and characterize samples, including low-molecular-mass molecules, prevailingly as guest of the host crystalline phase. The molar ratio between styrene monomeric units

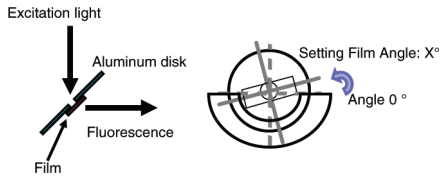

Figure 3. Setting way of sample films for the measurements of polarized fluorescence together with the definition of setting film angle. In the case of UPA1 and UPA2, the stretching direction is 0°.

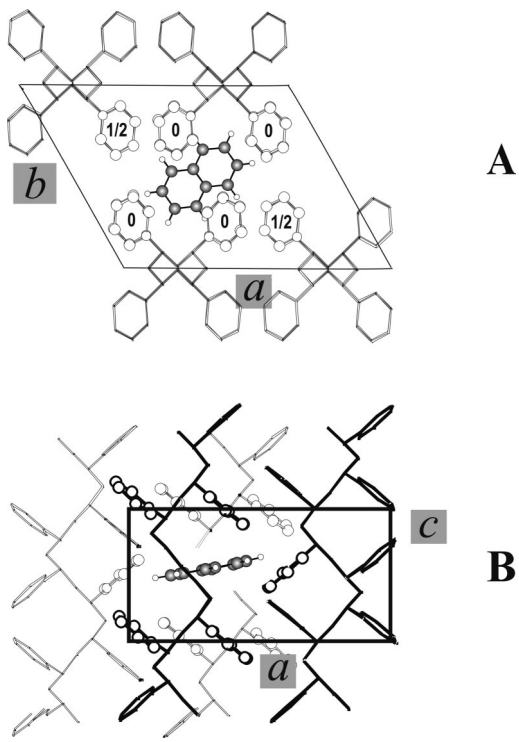

Figure 4. Model of packing and unit cell for the crystal structure of the sPS/NP clathrate co-crystalline phase, presenting the calculated minimum energy location of naphthalene. In particular, the unit cell is shown for two different views, along *c* axis (A) and perpendicular to the *ac* plane (B). The 10 phenyl rings that confine the cavity or the NP guest are represented by stick and balls.

and cavities for the delta crystalline phase is 4:1. Because the crystallinity is about 40%, the molar ratio between styrene monomeric units and cavities of the sPS films is not far from 10:1.

The fraction of NP molecules in the co-crystalline phase and in the amorphous region could not always be determined so exactly. When I0 and I90 of NP are measured by rotating a film containing NP around the excitation light, each I0 or I90 of NP should be the same at any setting angles when NP molecules are in amorphous region because of their random distribution. However, if co-crystalline phase of sPS/NP is oriented with high regularity, the angular distributions of I0 and I90 of NP should appear like Figure 11, where the minimum values of I0 and I90 of NP in co-crystalline phase are 0, respectively. The isotropic intensity of I0 and I90 in Figure 11 is assumed to be mainly from NP molecules in the amorphous region. Thus, the ratio between highest I0 (≈3000) and the isotropic intensity of I0 (≈1300) suggests the amount of NP in the amorphous region is less than 50% to first approximation, while the fraction of NP in the co-crystalline phase is higher than 55% (≈(3000 − 1300)/3000) of all the NP molecules in the film.

X-ray Diffraction Measurements. Wide-angle X-ray diffraction patterns with nickel filtered Cu Kα radiation were obtained, in reflection, with an automatic Philips diffractometer as well as, in transmission, by using a cylindrical camera (radius = 57.3 mm). In the latter case the patterns were recorded on a BAS-MS Imaging Plate (FUJIFILM) and processed with a digital imaging reader (FUJIBAS 1800).

In particular, to recognize the kind of crystalline orientation present in the samples, photographic X-ray diffraction patterns were taken by placing the film sample parallel to the axis of the cylindrical camera and by sending the X-ray beam parallel or perpendicular to the film surface. The degree of axial orientation, that is, of preferential parallel orientation of the axes of the crystalline helices with respect to the film stretching direction, has been evaluated by using the Herman's orientation function:

$$f_c = (3\overline{\cos^2 x} - 1)/2 \tag{4}$$

by assuming $\overline{\cos^2 x}$ as the squared average cosine value of the angle, x, between the draw direction and the crystallographic c (chain) axis. The orientation factor, f_c, is equal to 1 for perfect alignment ($x = 0°$), whereas it is equal to −0.5 for perpendicular alignment ($x = 90°$). For random orientation $\overline{\cos^2 x}$ is 1/3, and hence f_c is zero.

The degree of the $a_{||}\, c_{||}$ uniplanar orientation of the crystallites with respect to the film plane has been formalized on a quantitative numerical basis using Hermans' orientation functions,[26] in analogy to that one defined for the axial orientation:

$$f_{010} = (3\overline{\cos^2 x_{010}} - 1)/2 \tag{5}$$

by assuming $\overline{\cos^2 x_{010}}$ as the squared average cosine value of the angle, x_{010}, between the normal to the film surface and the normal to the (010) crystallographic plane.

Because, in our cases, a θ_{010} incidence of X-ray beam is used, the quantity $\overline{\cos^2 x_{010}}$ can be easily experimentally evaluated

$$\overline{\cos^2 x_{010}} = \overline{\cos^2 \chi_{010}} = \frac{\int_0^{\pi/2} I(\chi_{010}) \cos^2 \chi_{010} \sin \chi_{010} d\chi_{010}}{\int_0^{\pi/2} I(\chi_{010}) \sin \chi_{010} d\chi_{010}} \tag{6}$$

where $I(\chi_{010})$ is the intensity distribution of a (010) diffraction on the Debye ring and χ_{010} is the azimuthal angle measured from the equator.

The diffracted intensities $I(\chi_{010})$ of eq 6 were obtained by using an AFC7S Rigaku automatic diffractometer (with a monochromatic Cu Kα radiation), and were collected sending the X-ray beam parallel to the film surface and maintaining an equatorial geometry. Because the collection was performed at constant 2θ values and in the equatorial geometry, the Lorenz and polarization corrections were unnecessary.

In these assumptions, f_{010} is equal to 1 and −0.5 if (010) planes, that is, *ac* planes, of all crystallites are perfectly parallel and perpendicular to the plane of the film, respectively.

Fluorescence Depolarization Technique. Fluorescence spectra and fluorescence depolarization were measured at 25°C on a Hitachi F-4500 spectrofluorometer. All the sPS films and a PVAc film containing NP were stuck on an aluminum disk being 0.5 mm thick with a circle hole whose diameter is 2.0 mm in order to irradiate the exact same part no matter how the film was rotated. Fluorescence measurements of films were carried out by placing the films on aluminum disks set in a holder shown in Figure 3. Thin sPS films containing NP on quartz disks prepared by using a spin-coating method were set in a holder directly. Films were rotated by every 10° in the same plane whose center was at 45° to the exciting beam. In particular, in the case of UPA1 and UPA2, the stretching direction was determined to be 0°. In other cases, 0° does not mean anything at all. To measure NP polarized fluorescence, a Hitachi automatic polarizer was attached to a Hitachi F-4500 spectrofluorometer. Excitation wavelength was 280 nm. The I0 and I90 values were determined by averaging the polarized fluorescence intensities around 337 nm peak (16 points) measured repeatedly: two or three times each for one angle from 0 to 360° and again from 360 to 0°. Thus, the I0 and I90 values are the average of at least 64 data.

Computational Methods (Molecular Dynamics). The polymer starting structure was that one determined by X-ray diffraction

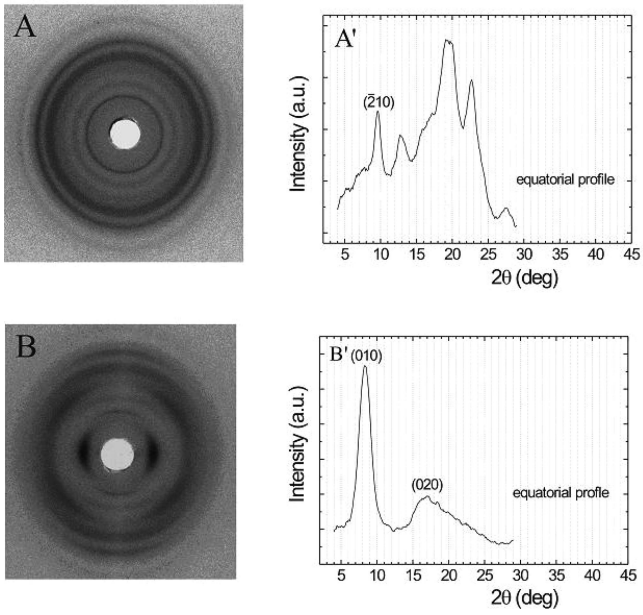

Figure 5. X-ray diffraction patterns (Cu Kα) of the sPS/NP clathrate film with 2 wt % of NP prepared by the same method as UP1 and UP2, exhibiting $a_{||}$ $c_{||}$ uniplanar orientation, taken with beam perpendicular (through, A) and parallel (edge, B) to the film plane and collected on a photographic cylindrical camera, for film placement parallel to the axis of the camera. The digital reading of the equatorial profiles of the patterns A and B are reported in A′ and B′, respectively.

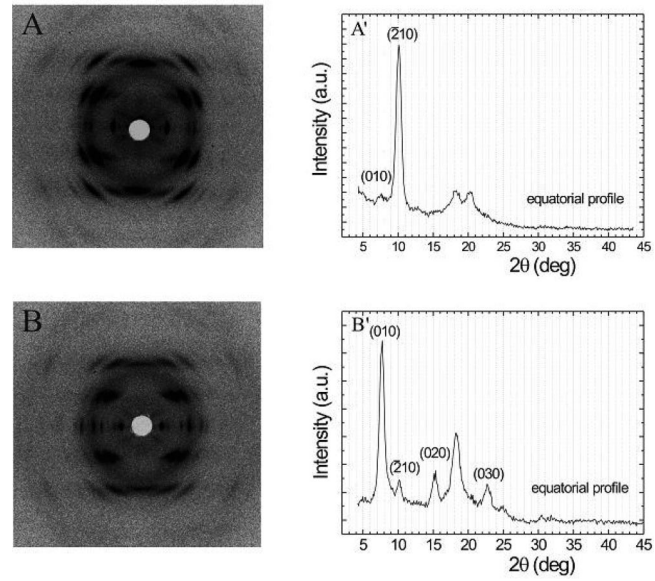

Figure 6. X-ray diffraction patterns (Cu Kα) of the sPS/NP clathrate with 5 wt % of NP film prepared by the same method as UPA1 and UPA2, exhibiting $a_{||}$ $c_{||}$ uniplanar-axial orientation, taken with beam perpendicular (through, A) and parallel (edge, B) to the film plane and collected on a photographic cylindrical camera, for film placement parallel to the axis of the camera. The digital reading of the equatorial profiles of the patterns A and B are reported in A′ and B′, respectively.

studies.[19a] In order to save considerable computer time, we applied orthorhombic periodic boundary conditions using a procedure developed by some of us. The monoclinic *a* and *c* crystal vectors coincide with the Cartesian *x* and *z* directions of the simulation box, respectively. The *y* direction of the simulation box forms an angle θ of 27° with the *b* axis and is perpendicular to the *ac* plane. In this way, the monoclinic periodic replication properties of the unit cell could be obtained by *quasi-orthorhombic* boundary conditions. The simulated host polymer contains 3072 atoms. A total of seven penetrating molecules were placed into host cavities. The system was equilibrated for 500 ps and then sampled for 1 ns. Molecular dynamics simulations were run at constant temperature (300 K) and pressure (1 atm). All simulations were monitored to check for good convergence in terms of energy, temperature, and density, among other properties.

Results and Discussion

Uniplanar and Uniplanar-Axial Orientation of the Polymer Co-Crystalline Phases. Figure 4 shows the unit cell of the sPS/NP clathrate phase, where the unit cell has been obtained by X-ray diffraction data while the guest location and orientation by molecular modeling.[8] The two different views are (A) along *c* axis and (B) perpendicular to the *ac* plane, respectively. The 10 phenyl rings that confine the NP guest are represented by stick and balls.

Figures 5 and 6 show that X-ray diffraction patterns of films having sPS/NP clathrate phase prepared in the exactly same manner as UP1 (UP2) and UPA1 (UPA2), respectively: they were taken with beam perpendicular (through) and parallel (edge) to the film plane and collected on a photographic cylindrical camera. An intense (2̄10) reflection (at $2\theta_{\text{Cu K}\alpha} = 10.2°$) clearly indicates the formation of the clathrate sPS/NP phase.[8,10,19]

As for the film obtained by chloroform solution casting (like UP1 and UP2 of Table 1), the edge pattern (Figure 5B) shows a very intense equatorial arc corresponding to the (010) reflection (at $2\theta_{\text{Cu K}\alpha} = 8.2$). This clearly indicates that, as usually observed[25−27] for guest-exchange processes in sPS co-crystals,[32] the (010) uniplanar orientation, that is, the orientation of the *ac* plane (shown in Figure 4B) parallel to the film plane is fully maintained. The position of this peak, intermediate between that one of a completely filled sPS/NP clathrate ($d = 1.15$ nm, $2\theta_{\text{Cu K}\alpha} = 7.7°$)[8] and that one of the empty δ phase ($d = 1.05$ nm, $2\theta_{\text{Cu K}\alpha} = 8.4°$)[19a] is of course related to the low guest content.

On the other hand, the through pattern (Figure 5A) shows only Debye-Sherrer rings, indicating the absence of axial orientation in the film plane. This information, also present in the corresponding equatorial profiles of Figure 5A′ and B′, clearly confirms the occurrence of the $a_{||}$ $c_{||}$ uniplanar orientation for the cast sPS/NP clathrate film. The corresponding degree of uniplanar orientation has been evaluated as $f_{010} \approx 0.75$.

As for the uniaxially stretched film (like UPA1 and UPA2 of Table 1), both through (Figure 6A) and edge (Figure 6B) patterns, present essentially only equatorial reflections (at $2\theta_{\text{Cu K}\alpha} = 7.7$, 10.2, 15.3, 18.5, and 23.1°) as is typical of axially oriented samples, with reflection arcs centered on layer lines, whose periodicity is determined by the periodicity of the polymer helix (0.78 nm for the s(2/1)2 sPS helix). However, as shown by the visual inspection of the photographic patterns (Figure 6A,B) and in a more clear way by the digital reading of their equator (Figure 6A′ and B′, respectively), the relative intensities of the reflections are completely different for the two patterns. In particular, in the through pattern (Figure 6A and A′) the (010) reflection is barely detectable, while the (2̄10) reflection is the most intense peak. On the other hand, in the edge pattern (Figure 6B,B′) the (010) is the most intense, while the (2̄10) reflection is weak. Quantitative evaluations show that the degree of axial orientation f_c is higher than 0.9, while the degree of $a_{||}$ $c_{||}$ uniplanar orientation is not far from 0.7.

In summary, cast films (like UP1 and UP2 of Table 1) present a high degree of $a_{||}$ $c_{||}$ uniplanar orientation, which is schematically shown in Figure 7A. The stretched films (like UPA1 and UPA2 of Table 1) present a very high degree of axial orientation (the *c* axis preferentially parallel to the stretching direction)

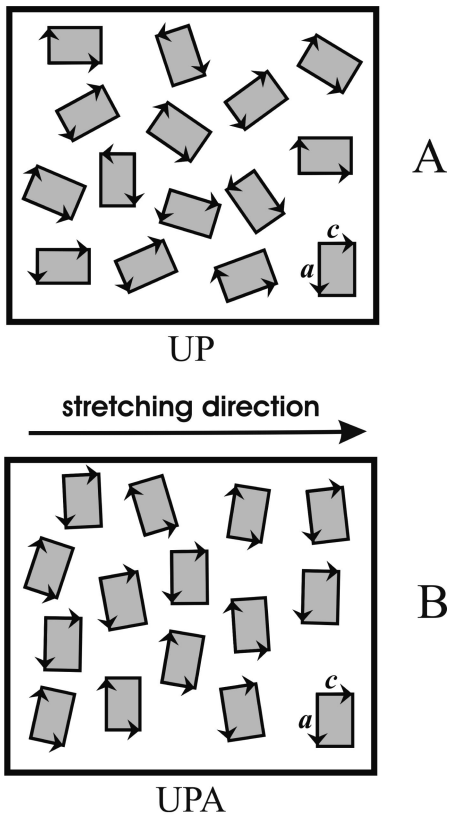

Figure 7. Sketch of the orientation of the sPS/NP co-crystals in the prepared films: (A) $a_{||}$ $c_{||}$ uniplanar orientation, that is, with *ac* crystalline planes preferentially parallel to the film plane (observed for films UP1 and UP2 of Table 1); (B) $a_{||}$ $c_{||}$ uniplanar-axial orientation, that is, with *ac* crystalline planes preferentially parallel to the film plane and *c* axes preferentially parallel to the stretching direction (observed for films UPA1 and UPA2 of Table 1).

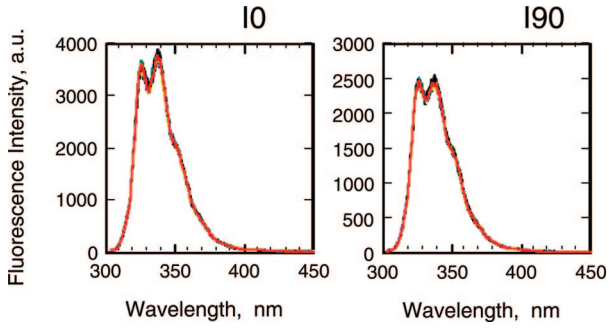

Figure 8. Fluorescence spectra of NP in aPS prepared by using a spin-coating method, I0 and I90 are the spectra of polarized fluorescence when the polarizers were set to measure I0 and I90. The spectra are for the setting film angle from 0° to 90°. The excitation wavelength was 280 nm.

associated with a rather high degree of $a_{||}$ $c_{||}$ uniplanar orientation, as schematically shown in Figure 7B. The latter films will be thereafter named as $a_{||}$ $c_{||}$ uniplanar-axial films. In this respect, it is worth noting that for the case of films with ideal uniplanar-axial orientation the crystallites cannot be further ordered except by decreasing their number by joining them into larger ones.[28]

Atactic Polystyrene (aPS) Films and Poly(vinyl acetate) (PVAc) Films Doped with NP. Figure 8 shows polarized fluorescence spectra of NP in aPS. The spectra for I0 and I90 are those obtained when two polarizers were set so as to measure I0 and I90, respectively. We rotated the films around the excitation light by every 10° from 0° to 90° and measured I0 and I90 of NP at each position of the film rotation. The spectra

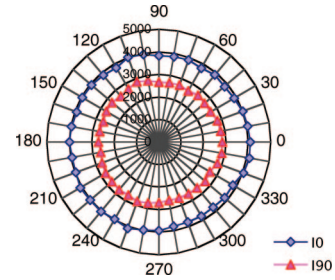

Figure 9. Angular distribution of I0 (◆) and I90 (▲) of NP in PVAc. The excitation wavelength was 280 nm.

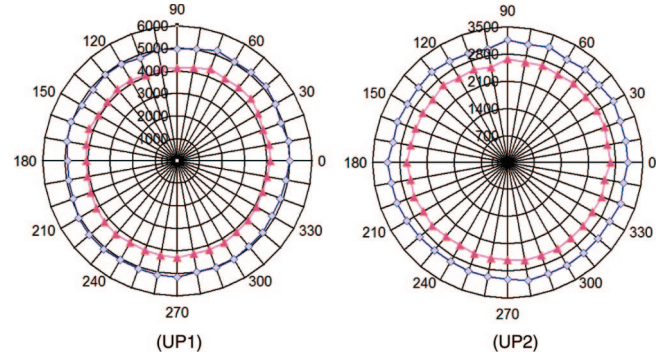

Figure 10. Angular distribution of I0 (◆) and I90 (▲) of NP in sPS/NP co-crystalline films having (010) uniplanar orientation (UP1 and UP2). The excitation wavelength was 280 nm.

were found to be perfectly identical with one another both in the cases of I0 and I90. This indicates that the NP molecules are distributed uniformly and randomly in the films.

Similar measurements were also conducted on NP molecules absorbed in PVAc films having a thickness similar to those of the sPS films of the next sections. Following to the paper by Nishijima et al., Figure 9 is shown in the circular polar coordinates, which is convenient to survey the changes of I0 and I90 with a rotation angle. The numbers around the outer circle show the angles of setting a film from 0 to 360° (=0°), while the distance from the center of the circle shows the intensity of polarized fluorescence I0 and I90. Figure 9 demonstrates that the angular distribution of I0 and I90 appears as a symmetric circle, although surfaces of thick films are uneven and as a consequence excitation light is more or less scattered. In any rate, it is no doubt that all the NP molecules are distributed isotropically all over the film.

sPS/NP Clathrate Crystalline Films UP1 and UP2. Figure 10 shows the angular distribution of I0 and I90 of NP in UP1 and UP2, that is, of films presenting an $a_{||}$ $c_{||}$ uniplanar orientation and no axial orientation. In spite of the different content of NP in UP1 and UP2 (2.4 and 7 wt %), the I90/I0 ratios were found to be extremely similar, namely, 0.83 (UP1) and 0.84 (UP2). Moreover, the average values of fluorescence anisotropy (r) for all the angles were almost identical for UP1 (0.052) and UP2 (0.054). The nearly identical values of I90/I0 and r suggest that the distributions of NP molecules between the amorphous and the crystalline phases are quite similar for UP1 and UP2. Thus, the preparation method of UP1 and UP2 is ascertained to be quite reproducible.

The presently observed r values are a little smaller than the r value of NP in an aPS film where mobility of NP and transportation of excitation energy can be neglected.[8a] However, as already discussed in our previous paper,[8a] this relatively low anisotropy values do not indicate that NP guest molecules are mobile: here the motion is not referred to translational diffusion but to local molecular mobility such as rotational motion. The

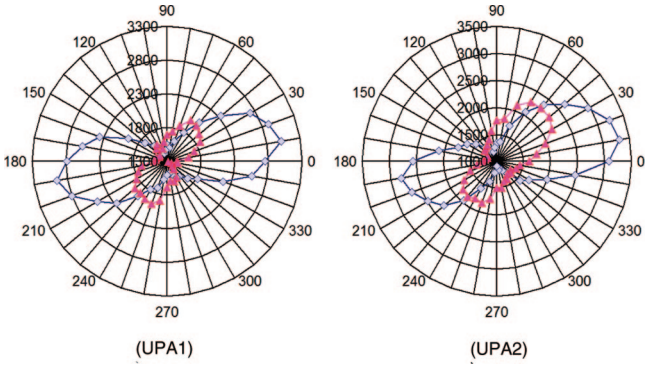

Figure 11. Angular distribution of I0 (◆) and I90 (▲) of NP in sPS/NP co-crystalline films prepared by stretching procedures and having $a_{||}$ $c_{||}$ uniplanar-axial orientation (UPA1 and UPA2). The excitation wavelength was 280 nm.

observed *r* values of NP are rather close to the *r* values of NP in the fibril region of sPS/chloroform gels (∼0.06)[33] and isotactic polystyrene/*cis*- and *trans*-decalin gels (∼0.06),[34] which are assumed to be reasonable for immobile guest molecules. In fact, ^{2}H NMR studies on sPS samples have shown that the local molecular mobility of aromatic compounds is reduced when they are guest of the nanoporous δ phase rather than dissolved in the amorphous phase.[35] In particular, the local mobility of the large NP guest molecule is restricted at least at room temperature.[35b] This restricted NP mobility is quite reasonable because its molar volume (127 Å^3) is close to the volume of the cavity (∼120−160 Å^3).[19b]

In agreement with the absence of axial orientation, the figures in the circular polar coordinates demonstrate that the distribution of all the NP molecules is uniform. In fact, the *c* axes of the sPS/NP crystallites are randomly distributed in the film plane, while the *ac* planes of crystallites are preferentially parallel to the surface of the film (Figure 7A). Most NP molecules in clathrate crystalline regions are considered to take their molecular plane orientation almost perpendicular (Figure 4B) and their long axis almost parallel (Figure 4A) to the film plane. However, because the *ac* planes, although parallel to the film plane, for different crystallites are randomly rotated in the film plane, the I0 and I90 should not be dependent on the angle of film rotation.

sPS/NP Clathrate Crystalline Films UPA1 and UPA2. Figure 11 shows the angular distribution of I0 and I90 of NP for the films UPA1 and UPA2, presenting a $a_{||}$ $c_{||}$ uniplanar-axial orientation of the sPS/NP clathrate phase. For the crystallites the *c* chain axes are preferentially parallel to the stretching direction and the *ac* planes are preferentially parallel to the surface of the film. The stretching directions of UPA1 and UPA2 were set to be 0° as the rotational angles of the films.

Both the figures in the circular polar coordinates of Figure 11 after Nishijima's papers[9] demonstrate that the distribution of NP molecules is not uniform and isotropic. The shape of the distribution of UPA2 is roughly similar to that of UPA1, although it unfortunately shows an asymmetrical shape. This asymmetry of the intensities of polarized fluorescence observed for UPA2 is due to a sort of waving of UPA2 film. The waving surface induces stronger light scattering. Because the scattering light is polarized, the apparent intensities of I0 and I90 would depend on the rotation angle of the film.

On the contrary, UPA1 showed perfect symmetric lines by rotation of the film around the excitation light between 0 and 360°. It is very interesting that the maximum values of I0 appeared at 10° and 190° while the maximum values of I90 appeared at around 60° and 240°. The center of circle figure of UPA1 shown in Figure 11 is 1300. This means that NP molecules with a fluorescence intensity of 1300 are distributed toward all the directions. These NP molecules can be dissolved in the amorphous region or can be guest of sPS/NP crystallites, being unoriented or presenting only uniplanar or only axial orientation. Thus, the NP molecules, except the ones showing the fluorescence intensity of 1300, present high regularity in their three-dimensional orientation, all over the film. These ordered NP molecules can be assumed to be guest of the sPS/NP co-crystalline phase with uniplanar-axial orientation. Now that we have obtained a special film where sPS/NP clathrate phase has almost unique arrangement all over the film, we have tried to determine the three-dimensional arrangement of a guest NP molecule in the co-crystalline unit-cell by using the angular distributions of I0 and I90 shown in Figure 11 (UPA1).

Fitting of the Angular Distribution of I0 and I90 of NP in UPA1. It is worth noting that, for films presenting a purely axial orientation of the crystalline phase, the figures like Figures 9 and 10 are expected. Figure 11, showing non-uniform angular distribution of I0 and I90, is instead in agreement with the presence of uniplanar-axial orientation. Because the degree of axial orientation of the considered films is very high, most crystallites present their chain axes along the stretching direction.

We have tried to determine the three-dimensional arrangement of a guest NP molecule in the co-crystalline unit-cell able to reproduce the angular distributions of I0 and I90 shown in Figure 11 (UPA1). First, we defined three parameters, ***sc***, ***lc***, and ***sa***, which are the angles between the short (*s*) and long (*l*) axes of the NP guest molecule with the *c* and *a* axes of the host unit cell. We have changed the values of these three angles one by one by every 1° from 0° to 180°, and calculated each I0 and I90. Although all the crystallites present their chain (and *c*) axis orientation parallel to the stretching direction and the *ac* plane parallel to the film plane, the direction of *a* axes for each crystallite can be +90° or −90° against the stretching direction of the film (either upward or downward in Figure 7B). Thus, the I0 and I90 were obtained by averaging the calculated values for both cases. We assessed the validity of the trial fitting by minimizing the sum of the variance. When we set two angle values and changed another angle, good fitting turned out to appear near one angle. The best fitting of I0 and I90 can be obtained for ***sc*** ≈ ***lc*** ≈ 80° and for ***sa*** ≈ 105°. However, some sets of ***sc***, ***lc***, and ***sa*** were found to give the better fitting where the sum of the variance was nearly the same. Taking into account the results of the molecular modeling, the calculated values of I0 and I90 for ***sc*** = **lc** = 82° and for ***sa*** = 104° as an example are shown with the experimental values in Figure 12. To show clearly the fitting to reproduce the experimental data, Figure 12 is drawn in the Cartesian coordinates to demonstrate the angular distribution of I0 and I90, though the data are perfectly the same. The fitting reproduced the angles to have not only the maximum values but also small peak values of I0 and I90.

This guest orientation is compatible with the results of molecular dynamic simulations shown in Figure 13, as obtained for NP molecules in a crystal of δ form sPS. In fact, according to the molecular simulation, maximum probability for ***sc***, ***lc***, and ***sa*** would correspond to 85, 80, and 112°, respectively. Thus, the experimental data of I0 and I90 have allowed us to determine the orientation of the NP guest molecule with respect the axes of the co-crystal unit-cell (***sc*** ≈ ***lc*** ≈ 80° and for ***sa*** ≈ 105°), in satisfactory agreement with molecular modeling results.

Our previous paper described our trial to determine the location of the NP guest molecule in clathrate crystalline unit-cell by infrared dichroism measurements on axially oriented films.[8] Infrared dichroism measurements on axially oriented sPS co-crystalline films allow only to determine the angles between the crystalline chain axis and molecular axes.[23] Moreover, the evaluated angles between the NP molecules and the host *c* axis

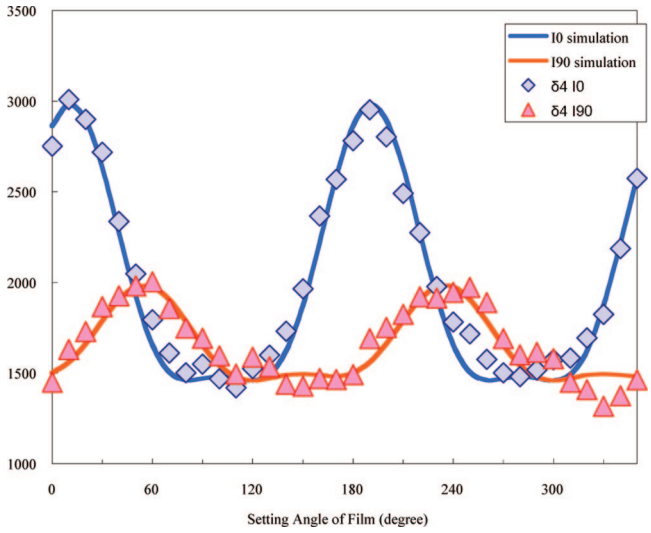

Figure 12. Fitting of the angular distribution of I0 (◆) and I90 (▲) of NP in the sPS/NP co-crystalline film, UPA1, whose values are the same as Figure 11. The solid lines show the fitting curves of I0 and I90 obtained for ***sc*** = 82°, ***lc*** = 82°, and ***sa*** =104°.

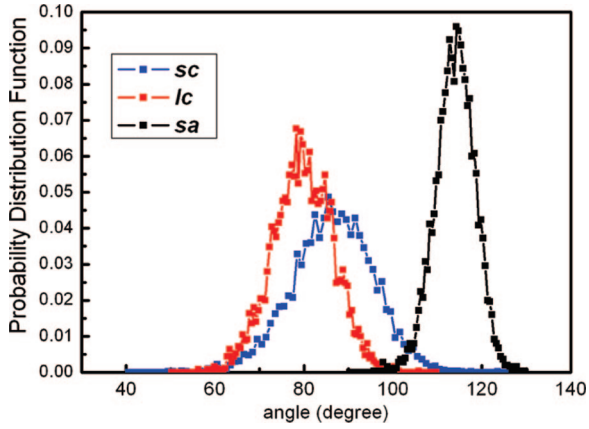

Figure 13. Naphthalene guest orientation in the nanoporous crystalline δ phase of sPS as derived by the molecular dynamics simulation. Angles ***sc***, ***lc***, and ***sa*** are the angles defined by the *a* and *c* crystalline axes of the polymer host and by the short (*s*) and long (*l*) in-plane symmetry axes of the naphthalene guest (see Figure 2A).

were substantially smaller than those obtained by molecular simulation. This deviation could be due to the vibrational mobility of the NP guest molecules with respect to their average location or more probably to the presence a fraction of NP molecules in the amorphous regions of the film, which (being generally unoriented) of course reduce the linear dichroism values.

The fluorescence method used in the present paper is much more efficient in determining the guest orientation in the polymer co-crystalline phase, with respect to the infrared method. In fact, the possible contribution from unoriented molecules possibly dissolved in the amorphous phase, rather than guest of the crystalline phase, can be easily removed (e.g., fluorescence below 1300 in Figure 11 for the UPA1 film). Note that the vibrational motion of the NP guest molecules that may affect infrared dichroism measurements does not influence I0 and I90 at all. As Nishijima pointed out,[9] some regular orientation patterns of guest molecules in films can never be distinguished by means of infrared dichroism measurements even if the arrangement is unique in the film, because infrared dichroism is only based on the process of absorption. It is needless to say but the angular distributions of I0 and I90 are obtained by way of both absorption and emission processes, thus this polarized fluorescence method can get more information.

Conclusions

The orientation of the clathrate co-crystalline phase of syndiotactic polystyrene with NP, in films prepared by solution casting and by NP treatments of axially stretched films, has been thoroughly characterized by X-ray diffraction measurements.

Films presenting the $a_{||}$ $c_{||}$ uniplanar and $a_{||}$ $c_{||}$ uniplanar-axial orientations of the sPS/NP co-crystalline phase have also been characterized by angular distribution of guest polarized fluorescence.

The reported fluorescence measurements clearly indicate that the uniplanar-axial orientation of the sPS/NP clathrate crystalline phase imposes a high three-dimensional regularity of the orientation of the guest molecules in whole film.

As a consequence, polarized fluorescence measurements for different film setting angles (the Nishijima's method) have allowed obtaining information on the orientation of guest NP molecules with respect to the polymer host crystalline axes. In particular, we have established by the fluorescence measurements that the angles formed by the short and the long axes of NP with the co-crystalline *c* axis are not far from 80°, while the angle between the short axis of NP and the co-crystalline *a* axis is nearly 105°, in satisfactory agreement with molecular dynamics simulations.

The fluorescence method used in the present paper is much more efficient in determining the guest orientation in the polymer co-crystalline unit-cell with respect to the infrared method. In fact, first of all, the possible contribution from molecules simply dissolved in the amorphous phase, rather than guest of the crystalline phase, can be easily removed. Moreover, the use of films with uniplanar-axial orientation allows determining the orientation with respect to all crystalline axes, while the linear dichroism measurements allows determining the guest orientation only with respect to the crystalline axis aligned along the stretching direction. It is also worth adding that due to the high sensitivity of fluorescence measurements, the method can be applied also for very low degrees of occupancy of the crystalline cavities, that is, when the fluorescent guest molecules are present only in traces. In fact, the present fluorescence method can operate independently of the degree of occupancy of the crystalline cavities, for the whole range going from completely filled co-crystals to essentially empty nanoporous phases.

It is worth noting that this Nishijima's method has not been used at all, until now, due to the need of three-dimensionally oriented, rather than axially oriented, chromophore guests. The present results suggest that the Nishijima's method could be generally applied to guest fluorescent molecules of polymeric nanoporous crystalline phases as well as of polymer co-crystals, for which films with a uniplanar-axial orientation are available. In this respect it is worth adding that, for most semicrystalline polymers, stretching procedures suitable to achieve at least one kind of uniplanar-axial orientation can be found.[28]

Acknowledgment. This work was supported by Grant-in-aid for Scientific Research (C) (13650948) and (C) (15550183) from the Ministry of Education, Science, Sports and Culture of Japan. Financial support of the "Ministero dell'Istruzione, dell'Università e della Ricerca" of Italy, of "Regione Campania" (Centro di Competenza per le Attività Produttive), and of CINECA/INSTM (Progetti di Supercalcolo) is also acknowledged. The authors thank Prof. Haruto Ota and Prof. Hajime Torii of Shizuoka University and Dr. Paola Rizzo and Dr. Giuseppe Milano of University of Salerno for useful discussions.

References and Notes

(1) Itagaki, H.; Mita, I. In *Degradation and Stabilization of Polymers*; Jellinek, H. H. G., Ed.; Elsevier: Amsterdam, 1989; Vol. *2*, p 45.
(2) (a) Itagaki, H.; Horie, K.; Mita, I. *Prog. Polym. Sci.* **1990**, *15*, 361. (b) Itagaki, H.; Horie, J. *Rep. Prog. Polym. Phys. Jpn.* **2000**, *43*, 401.
(3) Itagaki, H. In *Experimental Methods in Polymer Science: Modern Methods in Polymer Research and Technology*; Tanaka, T., Ed.; Academic Press: New York, 2000; Chapter 3.
(4) Itagaki, H.; Umeda, Y. *Polymer* **1995**, *36*, 29.
(5) (a) Itagaki, H.; Inagaki, Y.; Kobayashi, N. *Polymer* **1996**, *37*, 3553. (b) Itagaki, H. *J. Lumin.* **1997**, *72*−*74*, 435. (c) Itagaki, H.; Kato, S. *Polymer* **1999**, *40*, 3501.
(6) Itagaki, H.; Arakawa, S. *Polymer* **2003**, *44*, 3921.
(7) Itagaki, H.; Ochiai, A.; Nakamori, T. *Eur. Polym. J.* **2006**, *42*, 1939.
(8) (a) Venditto, V.; Milano, G.; De Girolamo Del Mauro, A.; Guerra, G.; Mochizuki, J.; Itagaki, H. *Macromolecules* **2005**, *38*, 3696. (b) De Girolamo Del Mauro, A.; Carotenuto, M.; Venditto, V.; Petraccone, V.; Scoponi, M.; Guerra, G. *Chem. Mater.* **2007**, *19*, 6041.
(9) (a) Nishijima, Y.; Onogi, Y.; Asai, T. *J. Polym. Sci. C* **1966**, *15*, 237. (b) Nishijima, Y. *J. Polym. Sci. C* **1970**, *31*, 353.
(10) (a) Chatani, Y.; Shimane, Y.; Inagaki, T.; Ijitsu, T.; Yukinari, T.; Shikura, H. *Polymer* **1993**, *34*, 1620. (b) Chatani, Y.; Inagaki, T.; Shimane, Y.; Shikuma, H. *Polymer* **1993**, *34*, 4841. (c) De Rosa, C.; Rizzo, P.; Ruiz de Ballesteros, O.; Petraccone, V.; Guerra, G. *Polymer* **1999**, *40*, 2103. (d) Tarallo, O.; Petraccone, V. *Macromol. Chem. Phys.* **2005**, *206*, 672.
(11) (a) Petraccone, V.; Tarallo, O.; Venditto, V.; Guerra, G. *Macromolecules* **2005**, *38*, 6965. (b) Tarallo, O.; Petraccone, V.; Venditto, V.; Guerra, G. *Polymer* **2006**, *47*, 2402. (c) Malik, S.; Rochas, C.; Guenet, J.-M. *Macromolecules* **2006**, *39*, 1000. (d) Galdi, N.; Albunia, A.R.; Oliva, L.; Guerra, G. *Macromolecules* **2006**, *39*, 9171.
(12) (a) Iuliano, M.; Guerra, G.; Petraccone, V.; Corradini, P.; Pellecchia, C. *New Polym. Mater.* **1992**, *3*, 133. (b) De Rosa, C.; Petraccone, V.; Guerra, G.; Manfredi, C. *Polymer* **1996**, *37*, 5247. (c) Petraccone, V.; La Camera, D.; Pirozzi, B.; Rizzo, P.; De Rosa, C. *Macromolecules* **1998**, *31*, 5830. (d) Petraccone, V.; La Camera, D.; Caporaso, L.; De Rosa, C. *Macromolecules* **2000**, *33*, 2610. (e) La Camera, D.; Petraccone, V.; Artimagnella, S.; Ruiz de Ballesteros, O. *Macromolecules* **2001**, *34*, 7762. (f) Petraccone, V.; Esposito, G.; Tarallo, O.; Caporaso, L. *Macromolecules* **2005**, *38*, 5668. (g) Tarallo, O.; Esposito, G.; Passarelli, U.; Petraccone, V. *Macromolecules* **2007**, *40*, 5471.
(13) De Girolamo Del Mauro, A.; Loffredo, F.; Venditto, V.; Longo, P.; Guerra, G. *Macromolecules* **2003**, *36*, 7577.
(14) (a) Matsumoto, A.; Odani, T.; Sada, K.; Miyata, M.; Tashiro, K. *Nature* **2000**, *405*, 328. (b) Matsumoto, A.; Oshita, S.; Fujioka, D. *J. Am. Chem. Soc.* **2002**, *124*, 13749. (c) Oshita, S.; Matsumoto, A. *Chem.*−*Eur. J.* **2006**, *12A*, 2139. (d) Oshita, S.; Matsumoto, A. *Langmuir* **2006**, *22*, 1943.
(15) (a) Yokoyama, M.; Ishihara, H.; Iwamoto, R.; Tadokoro, H. *Macromolecules* **1969**, *2*, 589. (b) Point, J. J.; Coutelier, C. *J. Polym. Sci., Polym. Phys. Ed.* **1985**, *23*, 231. (c) Delaite, E.; Point, J. J.; Damman, P.; Dosière, M. *Macromolecules* **1992**, *25*, 4768. (e) Belfiore, L. A.; Veda, E. *Polymer* **1992**, *33*, 3833. (f) Paternostre, L.; Damman, P.; Dosière, M. *Macromolecules* **1999**, *32*, 153.
(16) (a) Guerra, G.; Vitagliano, V. M.; De Rosa, C.; Petraccone, V.; Corradini, P. *Macromolecules* **1990**, *23*, 1539. (b) Rizzo, P.; Albunia, A.R.; Guerra, G. *Polymer* **2005**, *46*, 9549. (c) Rizzo, P.; D'Aniello, C.; De Girolamo Del Mauro, A; Guerra, G. *Macromolecules* **2007**, *40*, 9470.
(17) (a) Manfredi, C.; Guerra, G.; De Rosa, C.; Busico, V.; Corradini, P. *Macromolecules* **1995**, *28*, 6508. (b) Loffredo, F.; Pranzo, A.; Venditto, V.; Longo, P.; Guerra, G. *Macromol. Chem. Phys.* **2003**, *204*, 859.
(18) (a) Reverchon, E.; Guerra, G.; Venditto, V. *J. Appl. Polym. Sci.* **1999**, *74*, 2077. (b) Ma, W.; Yu, J.; He, J. *Macromolecules* **2005**, *38*, 4755.
(19) (a) De Rosa, C.; Guerra, G.; Petraccone, V.; Pirozzi, B. *Macromolecules* **1997**, *30*, 4147. (b) Milano, G.; Venditto, V.; Guerra, G.; Cavallo, L.; Ciambelli, P.; Sannino, D. *Chem. Mater.* **2001**, *13*, 1506. (c) Tamai, Y.; Fukuda, M. *Polymer* **2003**, *44*, 3279. (d) Gowd, E. B.; Shibayama, N.; Tashiro, K. *Macromolecules* **2006**, *39*, 8412.
(20) (a) Rizzo, P.; Daniel, C.; De Girolamo Del Mauro, A. Guerra, G. It. Pat. N.SA2006A22. (b) Rizzo, P.; Daniel, C.; De Girolamo Del Mauro, A.; Guerra, G. *Chem. Mater.* **2007**, *19*, 3864. (c) Petraccone, V.; Ruiz de Ballesteros, O.; Tarallo, O.; Rizzo, P.; Guerra, G. *Chem. Mater.* **2008**, *20*, 3663.
(21) (a) Guerra, G.; Manfredi, C.; Musto, P.; Tavone, S. *Macromolecules* **1998**, *31*, 1329. (b) Guerra, G.; Milano, G.; Venditto, V.; Musto, P.; De Rosa, C.; Cavallo, L. *Chem. Mater.* **2000**, *12*, 363. (c) Musto, P.; Mensitieri, G.; Cotugno, S.; Guerra, G.; Venditto, V. *Macromolecules* **2002**, *35*, 2296. (d) Yamamoto, Y.; Kishi, M.; Amutharani, D.; Sivakumar, M.; Tsujita, Y.; Yoshimizu, H. *Polym. J.* **2003**, *35*, 465. (e) Venditto, V.; De Girolamo Del Mauro, A.; Mensitieri, G.; Milano, G.; Musto, P.; Rizzo, P.; Guerra, G. *Chem. Mater.* **2006**, *18*, 2205. (f) Daniel, C.; Sannino, D.; Guerra, G. *Chem. Mater.* **2008**, *20*, 577.
(22) (a) Larobina, D.; Sanguigno, L.; Venditto, V.; Guerra, G.; Mensitieri, G. *Polymer* **2004**, *45*, 429. (b) Annunziata, L.; Albunia, A. R.; Venditto, V.; Mensitieri, G.; Guerra, G. *Macromolecules* **2006**, *39*, 9166. (c) Albunia, A. R.; Minucci, T.; Guerra, G. *J. Mater. Chem.* **2008**, *18*, 1046.
(23) (a) Albunia, A. R.; Di Masi, S.; Rizzo, P.; Milano, G.; Musto, P.; Guerra, G. *Macromolecules* **2003**, *36*, 8695. (b) Albunia, A. R.; Milano, G.; Venditto, V.; Guerra, G. *J. Am. Chem. Soc.* **2005**, *127*, 13114. (c) Daniel, C.; Galdi, N.; Montefusco, T.; Guerra, G. *Chem. Mater.* **2007**, *19*, 3302.
(24) D'Aniello, C.; Rizzo, P.; Guerra, G. *Polymer* **2005**, *46*, 11435.
(25) (a) Rizzo, P.; Albunia, A. R.; Milano, G.; Venditto, V.; Guerra, G.; Mensitieri, G.; Di Maio, L. *Macromol. Symp.* **2002**, *185*, 65. (b) Rizzo, P.; Lamberti, M.; Albunia, A.R.; Ruiz de Ballesteros, O.; Guerra, G. *Macromolecules* **2002**, *35*, 5854. (c) C., Daniel; Avallone, A.; Rizzo, P.; Guerra, G. *Macromolecules* **2006**, *39*, 4820.
(26) (a) Rizzo, P.; Spatola, A.; De Girolamo Del Mauro, A.; Guerra, G. *Macromolecules* **2005**, *38*, 10089. (b) Albunia, A. R.; Annunziata, L.; Guerra, G. *Macromolecules* **2008**, *41*, 2683.
(27) (a) Rizzo, P.; Costabile, A.; Guerra, G. *Macromolecules* **2004**, *37*, 3071. (b) Rizzo, P.; Della Guardia, S.; Guerra, G. *Macromolecule* **2004**, *37*, 8043.
(28) (a) Heffelfinger, C. J.; Burton, R. L. *J. Polym. Sci.* **1960**, *47*, 289. (b) Werner, E.; Janocha, S.; Hopper, M.J.; Mackenzie, K.J. *Encycl. Polym. Sci. Eng.* **1986**, *12*, 193. (c) Rizzo, P.; Venditto, V.; Guerra, G.; Vecchione, A. *Macromol. Symp.* **2002**, *185*, 53.
(29) (a) Stegmaier, P.; De Girolamo Del Mauro, A.; Venditto, V.; Guerra, G. *Adv. Mater.* **2005**, *17*, 1166. (b) D'Aniello, C.; Musto, P.; Venditto, V.; Guerra, G. *J. Mater. Chem.* **2007**, *17*, 531.
(30) (a) Buono, A.; Rizzo, P.; Immediata, I.; Guerra, G. *J. Am. Chem. Soc.* **2007**, *129*, 10992. (b) Guadagno, L.; Raimondo, M.; Silvestre, C.; Immediata, I.; Rizzo, P.; Guerra, G. *J. Mater. Chem.* **2008**, *18*, 567.
(31) Daniel, C.; Galdi, N.; Montefusco, T.; Guerra, G. *Chem. Mater.* **2007**, *19*, 3302.
(32) (a) Uda, Y.; Kaneko, F.; Kawaguchi, T. *Macromolecules* **2005**, *38*, 3320. (b) Uda, Y.; Kaneko, F.; Kawaguchi, T. *Macromolecules* **2005**, *38*, 3380.
(33) Itagaki, H.; Mochizuki, J. *Macromolecules* **2005**, *38*, 9625.
(34) Itagaki, H.; Nakatani, Y. *Macromolecules* **1997**, *30*, 7793.
(35) (a) Trezza, E.; Grassi, A. *Macromol. Rapid Commun.* **2002**, *23*, 260. (b) Albunia, A. R.; Graf, R.; Guerra, G.; Spiess, H. W. *Macromol. Chem. Phys.* **2005**, *206*, 715.

MA801849B